

An Investigation of the Suitability Level of Palm Kernel Shell Ash Nanoparticles Thermal Coating on MS9001E Blades, for Hot Corrosion Resistance

Edeowede Abel Abhulimen¹, Thomas Ndyar Guma², Nnorom Achara³,
Shuaibu Ochetengwu Yakubu⁴

¹Mechanical Engineering Dept., Nigerian Defence Academy (NDA), Kaduna.

²Mechanical Engineering Dept., Nigerian Defence Academy (NDA), Kaduna,

³Mechanical Engineering Dept., Nigerian Defence Academy (NDA), Kaduna

⁴Mechanical Engineering Dept., Nigerian Defence Academy (NDA)

Corresponding Author: Edeowede Abel Abhulimen¹

ABSTRACT: Thermal Resistance and anti-corrosion tendency of MS9001E blade coated with palm kernel shell ash nanoparticles (PKSAnp) have been investigated. ATGA Q50 thermogravimetric analyzer and TA Instruments' universal analysis 2000 software were used to determine the thermogravimetric and the Differential thermal properties of the coated blades whereas the optimization process of the hot corrosion test was carried out using Taguchi approach of experiment design. The findings of the DTA/TGA scan of the PKSAnp show a lower proportion of breakdown after the sample was heated up to 1000°C which was minimally around 5% of the residual weight gained during heating. This is an indication that the PKSAnp is capable of withstanding temperature beyond 1000°C, being within the operating temperature of the gas turbine. The coated sample with 20g/l composition of the PKSAnp was found to perform best, as there was no noticeable weight loss at 1000°C but with 1.54% of the residual weight gained still retained. The response analysis shows evidence that the corrosion rate was lowered when the PKSAnp was raised from level 1 (substrate) to level 3 (20 g/l). This is probably due to the increased thickness of the composite slurry, preventing simple electron transmission from the anode to the cathode electrode. Analysis of surface response shows that although the corrosion rate decreased with a rise in PKSAnp to level 3, the time rose with level 3, reducing the corrosion with time above 2hrs which resulted in lower coating resistance at high temperature. A lower corrosion rate was achieved at level 3 (20g/l) PKSAnp, level 1 for time of 2hrs, level 1 (700°C) for temperature, and level 2 (40) for cycle, according to the complete interaction graphs of all four parameters. When compared with microstructure coated alloy, the hard PKSAnp nanostructured material has acquired the least corrosion rate. This indicates that the alloy has been largely shielded from the harsh corrosion environment by the PKSAnp covering.

Key Words: Palm Kernel Shell, Coating, Elevated Temperature, Hot Corrosion.

Date of Submission: 27-12-2024

Date of acceptance: 06-01-2025

I. INTRODUCTION

The blades of Gas Turbines (GT) are subjected to very strenuous environments inside the gas turbine, and operate under the most arduous conditions of temperature and stress than any component in the engine which often lead to blade failures and potentially destroying the engine. They also experience rapid temperature transients at various points during the engine cycle. The hot gases surrounding the blades are highly oxidizing and contain high levels of contaminants (like Sulphur and chlorine, if low-grade fuels are used). Increasing the engine operating temperature in order to maximize efficiency has resulted in the inability of the traditional corrosion resistant turbine blade alloys to last the expected minimum life. It is rare that an alloying element leads to enhancement both in high temperature strength and in hot corrosion resistance. It becomes more challenging to achieve both high temperature strength and hot corrosion resistance simultaneously from an alloying material, devoid of environmental toxicity. Whereas the use of inhibitors could be one of the best options for protecting the General Electric frame 9E (MS9001E) engine against corrosion, many corrosion inhibitors are prohibited due to their environmental toxicity.

High efficiency at elevated temperature can only be achieved with blades being thermally resistant and Thermal Resistance as a heat property refers to the temperature difference by which an object or a material resists heat flow. It is the inverse of thermal conductance [1] and is desirable in gas turbine blades in order for the engine to maintain high operating temperature. Corrosion as a phenomenon has existed for as long as

mankind and has wreaked havoc on several plants in the industrial age, bringing into focus the need to study and understand it. Being extractive metallurgy in reverse, it is the destructive and unintentional attack on metals [2]. Over the years, mankind has come to accept that corrosion is an inevitable part of the industrial process. The risk mounts with aging infrastructures thereby threatening lives and properties [3]. Although the coatings employed in gas turbine blades exhibit varying degrees of resistance to hot corrosion, there is an accelerated rate of oxidation of these coatings and substrates which occurs when a condensed phase is present on the surface[4].

II. MATERIALS AND METHODS

The methodology employed in this work includes the adoption of the PKSA Characterisation and the optimization of the coating composition in literature [5][6] and then subjecting the coated sample with optimum composition to; thermal analysis and hot Corrosion investigation.

2.1 Thermal Analysis

Using a TGA Q50 thermogravimetric analyzer, thermal decomposition was measured in terms of global mass loss. The device (see Plate 1) measured the mass loss as a function of temperature with a precision of 0.1. The samples were loosely placed in an open sample pan of 6.4mm diameter and 3.2mm depth with an initial sample weight of 8-10mg. With a heating rate of 10°C/min, the temperature was controlled to rise from room temperature (25°C) to 1000°C. At room temperature and atmospheric pressure, high quality Argon was constantly pumped into the furnace at a flow rate of 60ml/min. Argon was utilized to purge the furnace for 30mins before the commencement of each run to create an inert atmosphere and ward off any unintended oxidative breakdown. Using TA Instruments' universal analysis 2000 software, the TG and DTA curves were derived from TGA runs.



Plate 1: TGA Q50 thermogravimetric analyser

Differential scanning calorimetry (DSC) was the experimental method used to directly measure the difference in heat energy uptake in the samples relative to a reference, during a regulated temperature change carried out in a differential scanning calorimeter, in line with existing literature [7], [8], [9]. The method involved introducing heat energy into the sample cell and a reference cell simultaneously, while identically increasing the temperature of both cells over time. Due to difference in the composition of the sample and the reference, different amount of energy was required to raise the temperature of the cells. Thus, the excess amount of energy required to compensate for the temperature difference between the cells was measured and directly correlated to specific thermodynamic properties of the sample, as previously researched [10], [11]. Differential scanning calorimetry (DSC), being an analytical technique that measures the molar heat capacity of samples as a function of temperature, provided information about thermal stability, and structural “fingerprint” that was used to assess the structural conformation. It was performed using a differential scanning calorimeter that measures the thermal transition temperature (melting temperature; T_m) and the energy required to disrupt the interactions stabilizing the tertiary structure (enthalpy; ΔH) [12][13].

2.2 Hot corrosion test

The optimization process of the hot corrosion test was carried out using Taguchi approach of experiment design. The Taguchi method involves reducing the variation in a process through robust design of experiments. The overall objective of the method is to produce high quality product at low cost to the manufacturer. It is a method for designing experiments to investigate how different parameters affect the mean and variance of a process performance characteristic which defines how well the process is functioning. This experimental design involves using orthogonal arrays to organize the parameters affecting the process and the levels at which they should be varied instead of having to test all possible combinations. It therefore allows for the collection of the necessary data to determine which factors most affect product quality with a minimum amount of experimentation, thus saving time and resources [14]. The correlation impact of corrosion rate was assessed using an L9 Taguchi design of experiments. In this study; the sample condition, time, temperature and

cycle were the processing factors taken into account. The levels and parameters utilized in the investigation which were made feasible after first tests, are shown in

Table 1 whereas Table 2 demonstrates the construction of the L9 orthogonal array using the coding values.

Table 1: Factors and levels used in the work

Process Parameters	Level 1(1)	Level 2(2)	Level 3(3)
Samples (g/l)(A)	substrate	10	20
Time(hrs.)(A)	2	4	6
Temperature (°C)(C)	700	800	900
Cycle(D)	30	40	50

Table 2: Orthogonal array of Taguchi Experimental Design layout.

S/No	Samples	Time	Temperature	Cycle
1	1	1	1	1
2	1	2	2	2
3	1	3	3	3
4	2	1	2	3
5	2	2	3	1
6	2	3	1	2
7	3	1	3	2
8	3	2	1	3
9	3	3	2	1

The samples were tested in a molten salt environment (Na₂SO₄-60% V₂O₅) under

Table 1. Using a camel hairbrush, a uniformly thick coating of molten salt mixture (40 percent Na₂SO₄-60 percent V₂O₅) was applied to the sample that had been heated to 250°C. Before exposing these dried salt-coated specimens to hot corrosion tests which were carried out in a furnace, they were weighed. The salt-coated samples were stored in alumina boats before being placed in a muffle furnace set to 100°C for three to four hours to allow the salt to properly adhere and dry. An electronic weighing scale with a sensitivity of 0.01mg was used to record the combined weight of the boat and specimen at the conclusion of each cycle in the hot corrosion testing. Following the hot corrosion testing, FESEM/EDAX analysis was done on the samples, and comparative studies between the uncoated and the PKSA_{np}-coated specimens were conducted. The corrosion rate (CR) was calculated using Equation 1.

$$CR = 534W / DA t, \text{ mpy} \dots \dots \dots \text{Equation 1}$$

Where;

W is the weight loss in milligrams, D is the density in grams per cubic centimetre, A is the surface area in square inches, and t is the time in hours.

III. RESULT AND DISCUSSION

3.1 Thermogravimetric Analysis (TGA)/Differential Thermal Analysis (DTA)

The findings of the DTA/TGA scan of the PKSA nanoparticles are shown in Figure 1. The PKSA_{np}'s TGA curve shows a lower proportion of breakdown after the sample was heated up to 1000°C. The breakdown was minimally around 5% of the residual weight gained during heating, attributable to the vaporization of the water molecule present in the PKSA_{np}. The PKSA_{np} start decomposition from 100.28% to 100.23% at temperatures between 900°C and 1000°C. This could be attributed to the presence of carbon and SiO₂ in the materials. The maximum decomposition of the PKSA_{np} would occur at temperature beyond 1000°C. The residual weight stabilization, coincides with the silica content in PKSA_{np} at temperatures over 1000°C, as PKSA_{np} is more thermally stable as a result of the silica, which delayed the degrading process. This temperature of decomposition of the produced PKSA_{np} suggests that the materials could be used in the production of composites coating for blades operating at elevated temperature.

Figures 2 to 6 display the DTA/TGA of the coated blades with 0g/l, 5g/l, 10g/l, 15g/l and 20g/l respectively, of the PKSA_{np} composition used in the electrodeposition process. With 0g/l, there was a substantial weight loss of up to 52% at 1000°C, a decomposition that noticeably began at 450°C. 5g/l, 10g/l and 15g/l respectively experienced weight loss of 48%, 22% and 20% with noticeable decompositions beginning from 500°C, 600°C and 620°C respectively. However, the blade coated with 20g/l of PKSA_{np} (figure 6) was able to retain a weight of 101.54% at 1000°C. This implies that at that temperature, the residual weight gained was still being retained. This is an indication that for decomposition to occur, the component must be heated

beyond 1000°C, confirming the suitability of the coating for MS9001E whose operating temperature is within the range.

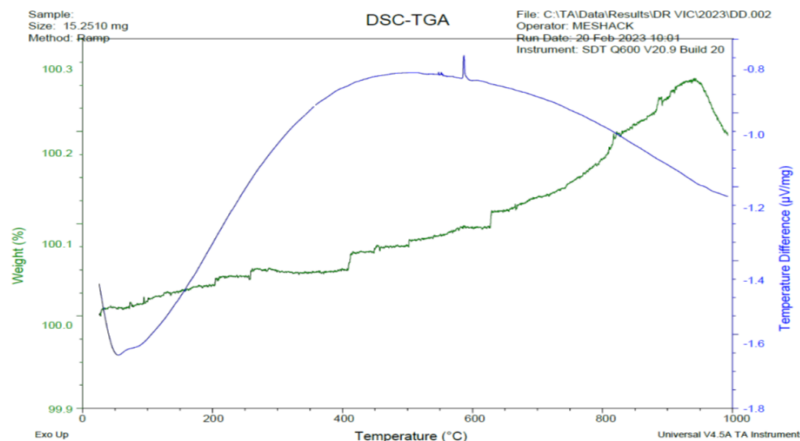


Figure 1: TGA/DTA of the PKSanp

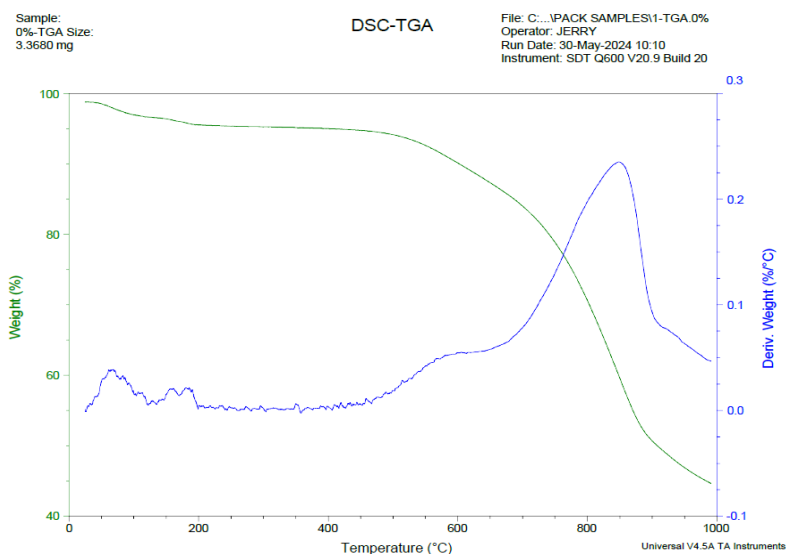


Figure 2: TGA/DTA of sample with 0g/l PKSanp

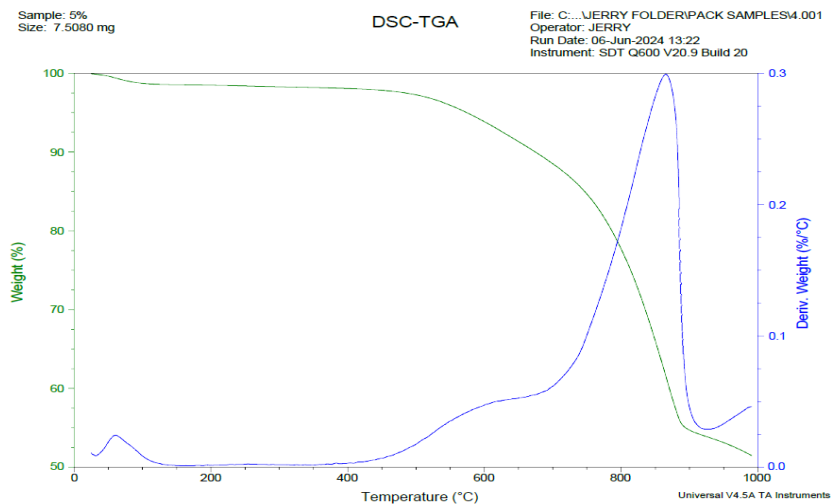


Figure 3: TGA/DTA of sample with 5g/l PKSanp

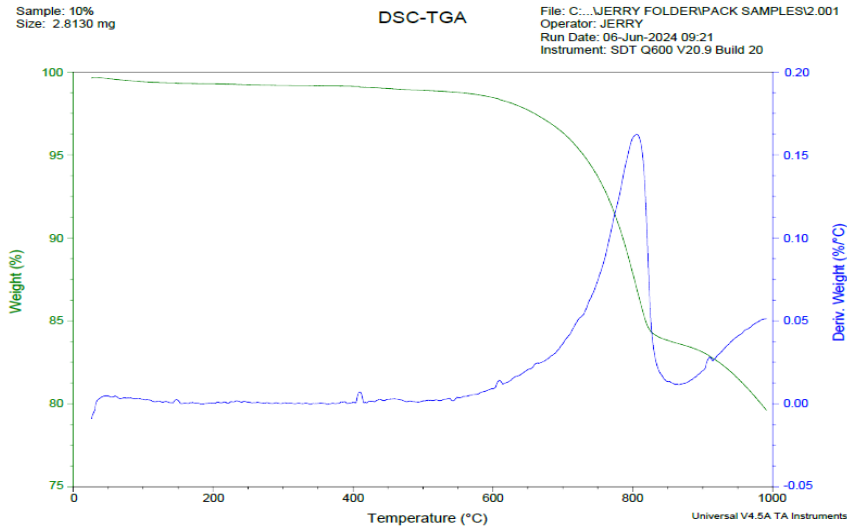


Figure 4: TGA/DTA of sample with 10g/l PKSAnp

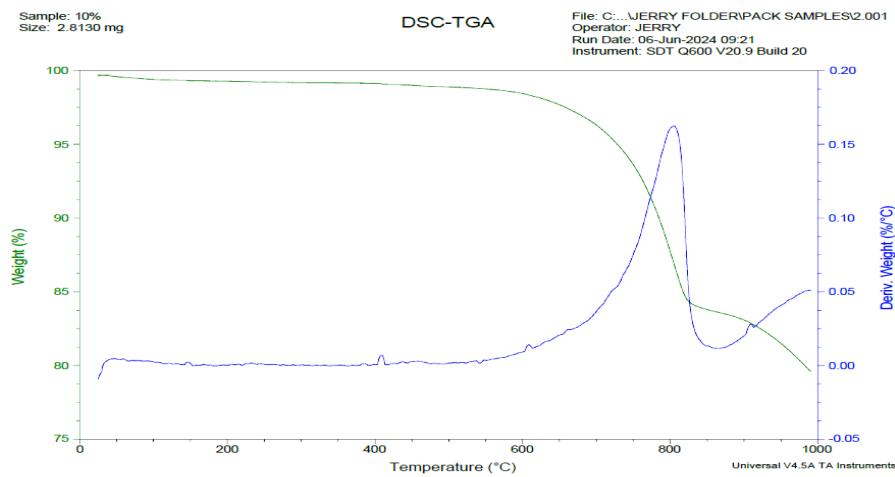


Figure 5: TGA/DTA of sample with 15g/l PKSAnp

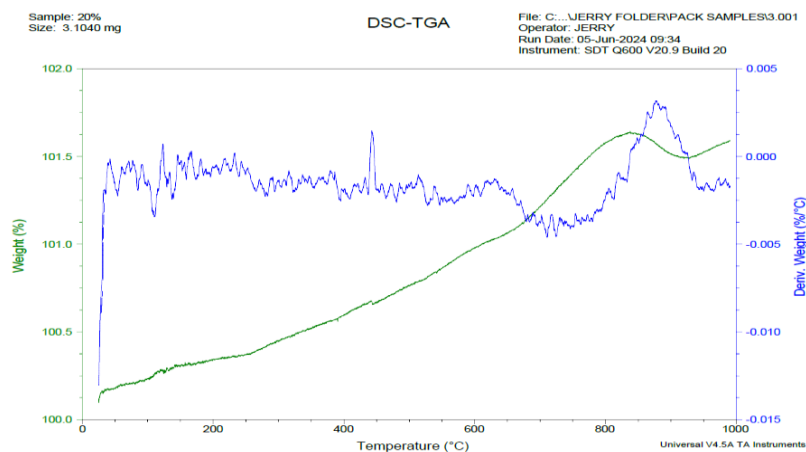


Figure 6: TGA/DTA of sample with 20g/l PKSAnp

3.2 Hot corrosion Analysis

The outcome of the L9 Taguchi technique responses is shown in Table 3 with equation 2 used to evaluate the signal to noise ratio (S/N). As already established, “the smaller the outcome, the better” [15].

$$S/N = -10 \cdot \log(\Sigma(Y^2)/n) \dots\dots\dots \text{Equation 2}$$

Where; Y = responses for the given factor level combination and n = number of responses in the factor level combination.

Table 3: Responses results of the Taguchi experiment(L9)

S/No	samples	time	Temperature	cycle	Corrosion rate(mpy)
1	1	1	1	1	1.55E+02
2	1	2	2	2	1.36E+02
3	1	3	3	3	2.39E+02
4	2	1	2	3	1.09E+02
5	2	2	3	1	1.29E+02
6	2	3	1	2	8.55E+01
7	3	1	3	2	4.54E+01
8	3	2	1	3	4.87E+01
9	3	3	2	1	9.53E+01

3.3 Mean to mean effect of the hot corrosion

The response analysis is discussed using Figure 7. It is evident from the figure that the corrosion rate was lowered when the PKSAnp was raised from level 1 (substrate) to level 3 (20 g/l). This is probably due to the increased thickness of the composite slurry, preventing simple electron transmission from the anode to the cathode electrode as established in previous literature [16]. The time rose from level 1 (2hrs) to level 3 (6hrs) as the corrosion rate increases. The lower corrosion rate is the outcome of increased PKSAnp deposition on the substrate surface at the ideal time of 2hrs. The corrosion rate was found to rise as the temperature of hot corrosion rose from level 1 (700°C) to level 3 (900°C). This indicates that increasing the temperature promotes faster PKSAnp dissolution, thereby raising corrosion rate and hardness values. However, the corrosion rate was decreased by increasing the cycle from level 1 (30) to level 4 (40) and a lengthy cycle of 50 reduced the coating corrosion resistance, thereby increasing the rate of corrosion.

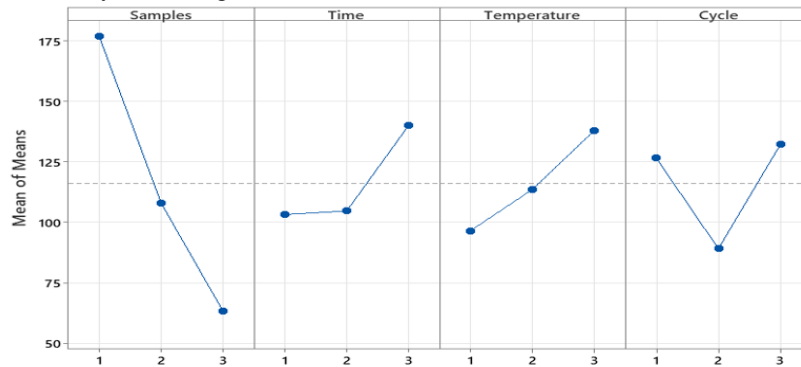


Figure 7: Plot of mean to mean of the four factors

3.4 Analysis of Surface Responses

The effects of the PKSAnp, time, temperature, and cycle on the corrosion rate were further discussed using Figures8-11, with the four elements under examination shown to have a good synergistic impact. The effective response of corrosion rate with PKSAnp and time is shown in Figure 8, while the effective response of corrosion rate with PKSAnp and temperature is shown in Figure 9. Both Figures show that although the corrosion rate decreased with a rise in PKSAnp to level 3, the time rose with level 3, reducing the corrosion. However, owing to hydrogen evolution, time above 2hrs was seen to result in lower coating resistance at high temperature, as in previous research [17]. The corrosion rate was found to increase with temperature and cycle as shown in Figure 10 whereas the corrosion rate with cycle and time shown in Figure 11, reveals corrosion increasing with time but fluctuating with cycle.

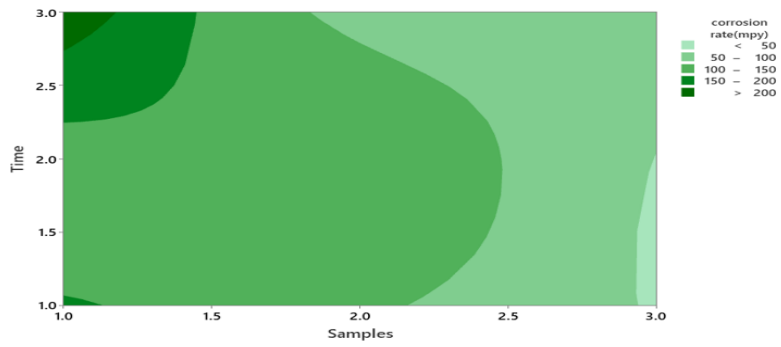


Figure 8: Contour plot of corrosion rate with PKSAnp and time

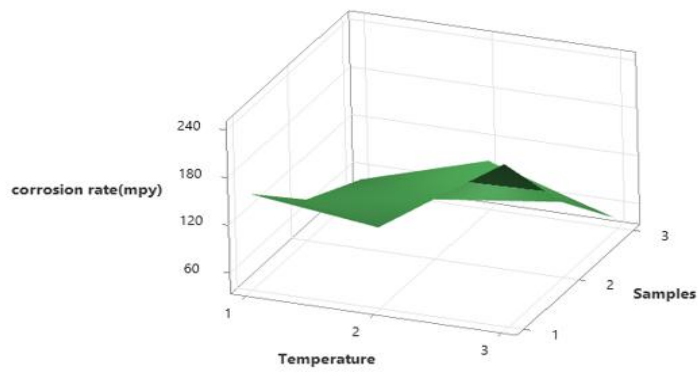


Figure 9: 3D plot of corrosion rate with PKSAnp and temperature

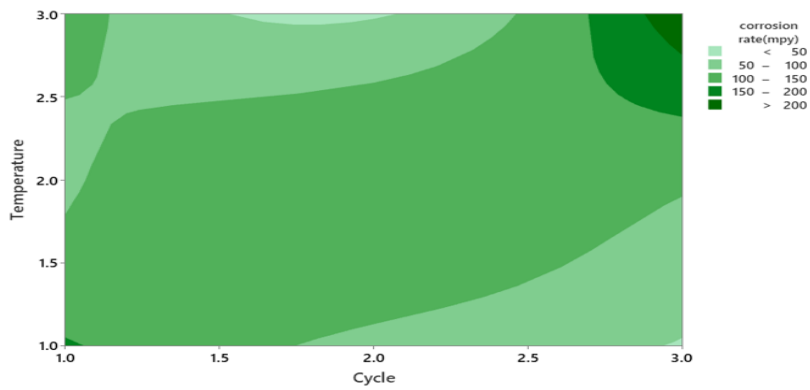


Figure 10: Contour plot of corrosion rate with temperature and cycle

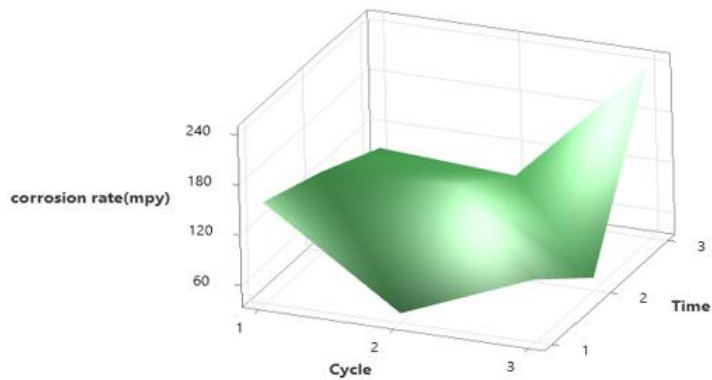


Figure 11: 3D plot of corrosion rate with cycle and time

IV. CONCLUSION

The TGA Q50 thermogravimetric analyzer and TA Instruments' universal analysis 2000 software as well as the Taguchi approach of experiment design has proven to be veritable tools in investigation/determination of coated blades' performance in elevated temperature and in hot corrosion. The findings show a lower proportion of PKSAnp breakdown after the sample was heated up to 1000°C. The breakdown was minimally around 5% of the residual weight gained during heating, attributable to the vaporization of the water molecule present in the PKSAnp. The coated sample with 20g/l composition of the PKSAnp was found to perform best, as there was no noticeable weight loss at 1000°C but with about 1.54% of the residual weight gained, still retained. The response analysis and analysis of surface response show a lower corrosion rate at level 3 (20g/l) PKSAnp, level 1 for time of 2hrs, level 1 (700°C) for temperature, and level 2 (40) for cycle. When compared with microstructure coated alloy, the hard PKSAnp nanostructured material has acquired the least corrosion rate which indicates that the alloy has been largely shielded from the harsh corrosion environment by the PKSAnp covering. It is therefore logical to infer that MS9001E blades coated with PKSAnp can operate effectively and sustainably at elevated temperature and in hot corrosion.

REFERENCES

- [1] Thermal resistance. Available: https://en.wikipedia.org/wiki/Thermal_resistance. Accessed: Oct. 04, 2021.
- [2] Abhulimen. E. A. (2018). "An investigation on the optimal concentration of oil palm (*elaeis guineensis*) leaves extract as corrosion inhibitor of carbon steel in deaerated saline solution," *MOJ Applied Bionics and Biomechanics*, vol.2, no.2, pp.109–113. doi: 10.15406/mojabb.2018.02.00050.
- [3] Gräfen H., Horn E.M., Schlecker H., and Schindler H. (2000). Corrosion. Ullmann's Encyclopaedia of Industrial Chemistry, Weinheim, Germany: Wiley-VCH Verlag GmbH &Co. KGaA., doi: 10.1002/14356007.b01_08.
- [4] Patarini V., Bornstein N. S., and DeCrescente M. A. (1979). "Hot corrosion of gas turbine components," *J Eng Gas Turbine Power*, vol.101, no.1, pp.177–185. doi: 10.1115/1.3446441.
- [5] Abhulimen E. A., Guma T. N., and Achara N. (2024). Characterization of Palm Kernel Shell Ash Nanoparticles as Coating Material for High Temperature Applications, *International Journal of Latest Technology in Engineering Management & Applied Science*, vol. 13, no.10, pp.93–98, Nov. 2024, doi: 10.51583/IJLTEMAS.2024.131012.
- [6] Abhulimen E. A., Guma T. N., and Achara N. (2024). "Optimization of *Elaeis Guineensis* Shell Ash Nanoparticles for Gas Turbine Blade Coating," *Engineering And Technology Journal*, vol. 9, no.12, pp. 5569–5578, Dec. 2024, doi: 10.47191/ETJ/V9I12.01.
- [7] Gill P., Moghadam T. T., and Ranjbar B., (2010). Differential Scanning Calorimetry Techniques: Applications in Biology and Nanoscience, *J Biomol Tech*, vol. 21, no. 4, p. 167,
- [8] Johnson C. M., (2013). "Differential scanning calorimetry as a tool for protein folding and stability," *Arch Biochem Biophys*, vol.531, no.1–2, pp.100–109, doi: 10.1016/j.abb.2012.09.008.
- [9] Wen J., Arthur K., Chemmalil L., Muzammil S., Gabrielson J., and Jiang Y. (2012). Applications of differential scanning calorimetry for thermal stability analysis of proteins: Qualification of DSC," *J Pharm Sci*, vol. 101, no. 3, pp. 955–964, doi: 10.1002/jps.22820.
- [10] Sturtevant J. M., (2003). Biochemical Applications of Differential Scanning Calorimetry, <https://doi.org/10.1146/annurev.pc.38.100187.002335>, vol.38, no.1, pp.463–488. doi: 10.1146/ANNUREV.PC.38.100187.002335.
- [11] Durowoju I. B., Bhandal K. S., Hu J., Carpick B., and Kirkitadze M., (2017). Differential Scanning Calorimetry — A Method for Assessing the Thermal Stability and Conformation of Protein Antigen," *J Vis Exp*, vol. 2017, no. 121, p. 55262. doi: 10.3791/55262.
- [12] Durowoju I. B., Bhandal K. S., Hu J., Carpick B., and Kirkitadze M. (2017). Differential Scanning Calorimetry-A Method for Assessing the Thermal Stability and Conformation of Protein Antigen," *J. Vis. Exp*, no. 121, Pp. 46262, doi: 10.3791/55262.
- [13] O'Neill M. J., (1966). Measurement of Specific Heat Functions by Differential Scanning Calorimetry, *Anal Chem*, vol. 38, no. 10, pp.1331–1336. doi: 10.1021/AC60242A011/ASSET/AC60242A011.FP.PNG_V03.
- [14] Design of Experiments via Taguchi Methods - Orthogonal Arrays. Accessed: Oct. 02, 2024. Available: https://eng.libretexts.org/Bookshelves/Industrial_and_Systems.
- [15] Abbas K. H., Thear T., Abdul R., and Ali M. K., (2021). Evaluation of Hot Corrosion Properties for Nano-coated Superalloy, *Journal of Applied Sciences and Nanotechnology*, Vol.1, No.1
- [16] Potter A., Sumner J., and Simms N., (2022). The effects of water vapour on the hot corrosion of gas turbine blade materials at 700°C," *Materials at High Temperatures*, vol. 39, no. 3, pp. 231–238. doi: 10.1080/09603409.2022.2056299.
- [17] Kanesund J., Brodin H., and Johansson S. (2020). High temperature corrosion influence on deformation and damage mechanisms in turbine blades made of IN-792 during service. *Eng Fail Anal*, vol. 110. doi: 10.1016/j.engfailanal.2020.104388.